

Article

Claudin-4 is required for AMPK-modulated paracellular permeability in submandibular gland cells

Ruo-Lan Xiang¹, Mei Mei², Xin Cong¹, Jing Li², Yan Zhang¹, Chong Ding³, Li-Ling Wu^{1,*}, and Guang-Yan Yu^{2,*}

¹ Center for Salivary Gland Diseases of Peking University School and Hospital of Stomatology, Department of Physiology and Pathophysiology, School of Basic Medical Sciences, Peking University Health Science Center and Key Laboratory of Molecular Cardiovascular Sciences, Ministry of Education, Beijing 100191, China

² Department of Oral and Maxillofacial Surgery, Peking University School and Hospital of Stomatology, Beijing 100081, China

³ Central Laboratory, Peking University School and Hospital of Stomatology, Beijing 100081, China

* Correspondence to: Li-Ling Wu, E-mail: pathophy@bjmu.edu.cn; Guang-Yan Yu, E-mail: gyyu@263.net

Tight junction plays an important role in mediating paracellular permeability in epithelia. We previously found that activation of AMP-activated protein kinase (AMPK) increased saliva secretion by modulating paracellular permeability in submandibular glands. However, the molecular mechanisms underlying AMPK-modulated paracellular permeability are unknown. In this study, we found that AICAR, an AMPK agonist, increased saliva secretion in the isolated rat submandibular glands, decreased transepithelial electrical resistance (TER), and increased 4 kDa FITC-dextran flux in cultured SMG-C6 cells. AICAR also induced redistribution of tight junction protein claudin-4, but not claudin-1, claudin-3, occludin, or ZO-1, from the cytoplasm to the membrane. Moreover, knockdown of claudin-4 by shRNA suppressed while claudin-4 re-expression restored the TER and 4 kDa FITC-dextran flux responses to AICAR. Additionally, AICAR increased ERK1/2 phosphorylation, and inhibition of ERK1/2 by U0126, an ERK1/2 kinase inhibitor, or by siRNA decreased AICAR-induced TER responses. AICAR induced the serine S199 phosphorylation of claudin-4 and enhanced the interaction of claudin-4 and occludin. Furthermore, pretreatment with U0126 significantly suppressed AMPK-modulated phosphorylation, redistribution, and interaction with occludin of claudin-4. Taken together, these results indicated that claudin-4 played a crucial role in AMPK-modulated paracellular permeability and ERK1/2 was required in AMPK-modulated tight junction barrier function in submandibular gland.

Keywords: AMP-activated protein kinase, claudin-4, tight junction, paracellular permeability, submandibular gland

Introduction

The salivary glands secrete saliva to lubricate the oral cavity, maintain the oral tissues, and initiate the process of digestion and an immune response against invaders that enter through the oral cavity (Ship, 2002). The secretion of saliva across salivary epithelium can be through either the transcellular or the paracellular pathway (Kawedia et al., 2007). The transcellular transport pathway in the salivary gland depends primarily on aquaporin 5 water channel localized on the luminal surface of acinar cells. Tight junctions are the cell–cell interactions that form a major barrier to the diffusion of materials through the paracellular pathway (Shen, 2012). Although most studies referring to the saliva secretion focus on the transcellular pathway through aquaporin channels (Frigeri et al., 2007), the

effect of tight junctions on the materials transport through paracellular pathway has recently received much attention. For example, emerging data show that cytokines, such as tumor necrosis factor- α (TNF- α) and interferon- γ (IFN- γ), alter tight junction structure and function. Cytokines-induced tight junction dysfunction is considered to be one of the major factors leading to the salivary gland destruction in Sjögren's syndrome (Ewert et al., 2010).

Tight junctions form the protein complex and play important roles in regulation of paracellular permeability, maintaining different cell domains and epithelial polarity. Tight junctions are composed of three types of components: transmembrane proteins (such as claudins and occludin), cytosolic scaffolding proteins (ZO-1), and cytosolic signaling proteins (Paris et al., 2008). Among these, claudins are the major transmembrane components of tight junctions. There are currently 27 claudin proteins that have been identified, each of which has a molecular weight of 20–27 kDa. They form the paracellular barrier that controls the flux of ions and small

molecules in the intercellular space between epithelial cells (Günzel and Yu, 2013). Claudin-1-deficient mice die soon after birth as a consequence of dehydration from transdermal water loss (Furuse et al., 2002). Claudin-2 constitutes leaky and cation (Na^+)-selective paracellular channels within tight junctions of mouse proximal tubules (Muto et al., 2010). Recent studies have shown that several human diseases are associated with the alteration of claudins (Günzel and Fromm, 2012). A variant of claudin-2 is associated with an overall increased risk of having Crohn's disease (Söderman et al., 2013). Claudin-3 and claudin-4 control tumor growth and metastases by sustaining expression of E-cadherin and limiting β -catenin signaling (Shang et al., 2012). Patients with claudin-19 mutations have a high risk of progression to chronic renal disease (Claverie-Martin et al., 2013). It has been clearly demonstrated that salivary glands have differential expression of claudin proteins. Human submandibular gland expresses claudin-1, -2, -3, -4, -5, -7, -11, and -16 (Maria et al., 2008). Rat submandibular gland expresses claudin-1, -3, -4, -5, and -7 (Peppi and Ghabriel, 2004). However, the precise role of each claudin in submandibular gland and the related regulatory mechanism remain to be elucidated.

AMP-activated protein kinase (AMPK) is a serine/threonine kinase that is evolutionarily conserved from yeast to mammals. AMPK is frequently reported being activated to deplete cellular ATP under stress conditions, such as nutritional deprivation, ischemia, hypoxia, oxidative stress, and so on (Kottakis and Bardeesy, 2012). Recently, it has been reported that tight junction formation induced by forskolin is likely mediated by the AMPK pathway in BeWo Cells derived from human choriocarcinoma (Egawa et al., 2008). Expression of a dominantly negative AMPK construct inhibits tight junction assembly in MDCK cells, and this response can be partially ameliorated by rapamycin (Zhang et al., 2006). The tight junction assembly is impaired when AMPK activity is downregulated using genetic manipulation strategy. These results suggest that activation of AMPK may involve in the regulation of tight junction function. Recently, we demonstrate that adiponectin increased saliva secretion of submandibular gland by modulating paracellular permeability through binding to adiponectin receptors and activation of AMPK (Ding et al., 2013). However, the mechanism of AMPK regulating tight junction of submandibular gland has not been clearly defined yet.

The present study was designed to explore the roles of activation of AMPK in modulating distribution of claudins and paracellular permeability, specially focusing on claudin-4 in salivary epithelium using SMG-C6 cell. The possible signaling pathway that mediated AMPK-induced claudin-4 redistribution in submandibular gland cells was also investigated.

Results

Activation of AMPK increases secretion of the isolated rat submandibular glands and paracellular permeability in SMG-C6 cells

To confirm the role of AMPK in the secretion of submandibular glands, we perfused 1 mM 5-aminoimidazole-4-carboxamide-ribonucleoside (AICAR), an AMPK activator, into the isolated rat submandibular glands for 30 min. Saliva flow was significantly

increased after AICAR administration (Figure 1A). The basal saliva flow was not changed in KRH perfusion group. Carbachol (1 μM), a muscarinic agonist, significantly increased saliva flow rate, which was used as the positive control. These results indicated that activation of AMPK increased the secretion of rat submandibular glands.

To further evaluate the effect of AMPK activation on the function of tight junction, the transepithelial electrical resistance (TER) was measured in SMG-C6 monolayer cells seeded onto polycarbonate filters. As an important indicator for the barrier function of tight junction, decreased TER is accompanied by increased paracellular permeability (Sáenz-Morales et al., 2009). In untreated SMG-C6 cells, the initial TER value was $592.67 \pm 29.84 \Omega\cdot\text{cm}^2$, which was consistent with previous studies in the same cell line and represented a relatively tight epithelium according to the description of electrical characteristics (Kawedia et al., 2008). AICAR (1 mM) induced a significant drop in TER values during 5–60 min. AICAR decreased TER values to 45.72% at 60 min compared with the control group ($P < 0.01$). In addition, incubation of SMG-C6 cells in a Ca^{2+} -free medium within 60 min, as a positive control, caused a dramatical decrease in TER values due to its effects on tight junction disassembly and paracellular opening as previously reported ($P < 0.01$) (Figure 1B). Because transcellular pathway might contribute to the net TER, we further measured the TER in K^+ -free medium that suppressed the Na^+/K^+ ATPase and thereby inhibited transcellular transport. As illustrated in Figure 1C, AICAR also induced a significant drop in TER values under the condition that transcellular transport was inhibited. After AICAR was removed, a quick recovery of TER was observed (Figure 1D). These results suggested that activation of AMPK increased paracellular permeability in the submandibular epithelia and the response might be associated with redistribution of tight junction proteins.

FITC-labeled dextran, a non-charged probe, passes across the epithelium through the paracellular route. It is widely used as a tracer for characterization of the permeability of paracellular water and macromolecule movement (Rosenthal et al., 2010). To further examine the biological effect of AMPK activation on tight junctions, we determined the permeability of 4 kDa FITC-dextran transporting across SMG-C6 cells from the apical to the basal side. The apparent permeability coefficients (Papp) for 4 kDa FITC-dextran were significantly enhanced by AICAR treatment for 10–60 min (Figure 1E). AICAR increased permeability of 4 kDa FITC-dextran by 81.59% at 60 min compared with the control group ($P < 0.01$). The flux result provided more evidence that AMPK increased paracellular permeability of submandibular gland cells.

Activation of AMPK induces redistribution of claudin-4

Recent studies in the cell biology of tight junctions indicate that the redistribution of claudins leads to significant changes in the tight junction structure and function in drosophila neural stem cells (Günzel and Fromm, 2012). In untreated SMG-C6 cells, claudin-1, -3, and -4 proteins were predominantly expressed in membrane, encircling the cells and delineating the cellular borders, while scarcely diffused in the cytoplasm (Figure 2A). To further confirm the intracellular location of claudin-1, -3, and -4

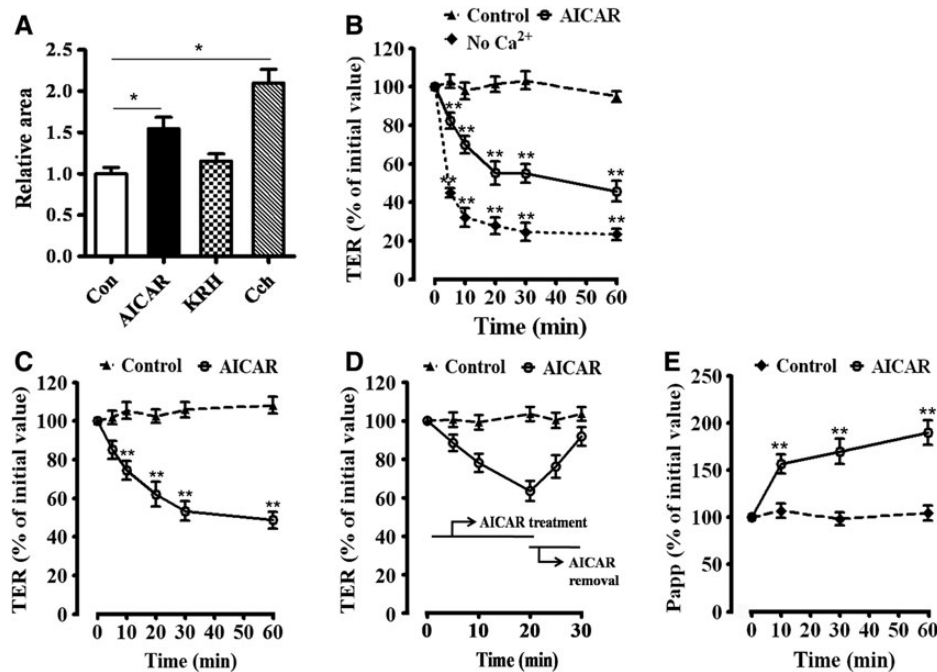


Figure 1 Activation of AMPK increases saliva secretion in the isolated rat submandibular glands and paracellular permeability of SMG-C6 cells. (A) *ex vivo* perfusion was performed in the isolated rat submandibular glands with 1 mM AICAR for 30 min. Saliva secretion was measured as the length of moisture on the filter paper. Carbachol was used as the positive control. (B) TER was measured by EVOM. SMG-C6 cells in a Ca²⁺-free medium were used as the positive control. (C) TER was measured under conditions where cell sheets were bathed in K⁺-free medium. (D) TER was measured after AICAR removal. (E) The apparent permeability coefficient (Papp) for 4 kDa FITC-dextran was performed to analyze transepithelial permeability of SMG-C6 cells. Values are mean \pm SD from three independent experiments. * $P < 0.05$ and ** $P < 0.01$ vs. control group.

proteins, sequential images of the monolayer of cells from the apical surface to the basal region along the z-axis were taken using confocal microscope. Consistently, claudin proteins were observed mainly in the lateral membranes of SMG-C6 cells. The double immunofluorescence staining showed that claudin-4 and ZO-1 were co-localized in the cell-cell borders of untreated SMG-C6 cells (Figure 2B). Claudin-4 immunoreactive signals along cell boundaries were elevated by AICAR treatment for 10, 30, and 60 min. The results indicated that claudin-4 was redistributed from the cytoplasm to the plasma membrane (Figure 2A). In contrast, AICAR did not induce redistribution of claudin-1 or claudin-3, other transmembrane component of tight junctions in SMG-C6 cells. These results suggested that AMPK selectively induced a redistribution of claudin-4, but not claudin-1 or claudin-3 in submandibular epithelial cells. We next determined the expression of claudin-4 in the rat submandibular gland tissue by immunofluorescence microscope. The images showed that claudin-4 was mainly expressed in the duct epithelial cells, and weakly presented in acinar cells (Figure 2C). The results suggested that claudin-4 might modulate the barrier function of duct and acinar cells in rat submandibular glands.

We extracted the cytoplasm and membrane fractions from the cells and performed western blot to evaluate the subcellular distribution of tight junction proteins. After AICAR treatment for 10 min, the concentration of claudin-4 was increased in the membrane fraction by 32.5% ($P < 0.05$) and decreased in the cytoplasm fraction by 21.2% ($P < 0.05$). On the other hand, the concentrations of

claudin-1, claudin-3, occludin, and ZO-1 in either cytoplasm or membrane fraction were not affected (Figure 2D–G). Western blot analysis further confirmed that AMPK selectively induced redistribution of claudin-4, but not claudin-1, claudin-3, occludin, or ZO-1.

To elucidate whether the distribution of claudin-4 is accompanied with changes in the expression level of claudin-4 in the SMG-C6 cells, we further determined the expression level of claudin-4 after AICAR treatment for 24 h in total-cell lysates. Western blot results showed that the level of claudin-4 did not change at 0.5, 1, and 24 h (Figure 2H). Furthermore, the levels of claudin-1, claudin-3, occludin, and ZO-1 did not change either (Figure 2H and I). Therefore, these data indicated that AMPK induced the claudin-4 redistribution, and did not change the expression level of claudin-4 over a 24-h period.

Depletion or re-expression of claudin-4 alters TER response induced by AMPK

To reveal the potential role of claudin-4 in paracellular permeability of SMG-C6 cells, we used specific shRNAs to knockdown the expression of claudin-4 (Figure 3A) and claudin-3 (Figure 3B), respectively. The depletion of claudin-4 slightly decreased the basal TER value by 15.64%, which was not statistically significant. Similarly, depletion of claudin-3 did not alter the basal levels of TER (Figure 3C). Then, we evaluated the AICAR-modulated paracellular permeability changes in these claudin-4 or claudin-3 knockdown cells. Compared with the scrambled control cells, AICAR-induced TER decrease was significantly inhibited in the claudin-4

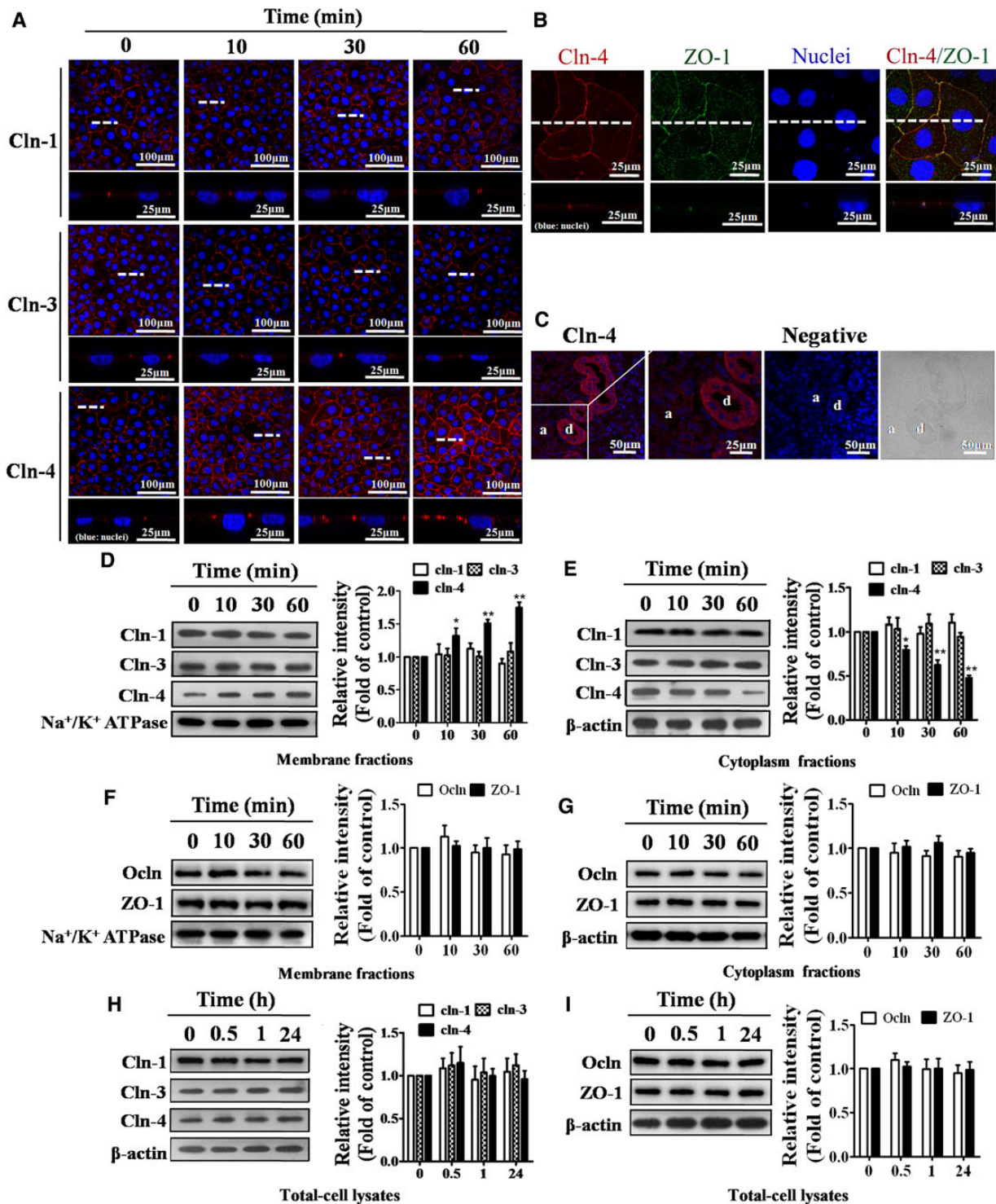


Figure 2 Distribution of claudin-1 (Cln-1), claudin-3 (Cln-3), and claudin-4 (Cln-4) in SMG-C6 cells after AICAR treatment. **(A)** Immunofluorescence images of claudin-1, -3, and -4 distribution in SMG-C6 cells at x–y planes and along the z-axis were taken after 1 mM AICAR stimulation at different time points. Each image is a representative of three separate experiments in duplicate. Scale bar, 100 and 25 μm for x–y and x–z images, respectively. **(B)** Co-immunofluorescence staining of claudin-4 with ZO-1 in SMG-C6 cells. Scale bar, 25 μm. **(C)** Expressions of claudin-4 proteins in rat submandibular glands were detected by immunofluorescence. Scale bar, 50 and 25 μm, respectively. a, acinus; d, duct. **(D–G)** Expressions of claudin-1, -3, -4, occludin, and ZO-1 proteins in membrane and cytoplasm fractions were detected by western blot analysis after 1 mM AICAR stimulation for different time points. **(H and I)** Expressions of claudin-1, -3, -4, occludin, and ZO-1 proteins in total-cell lysates of SMG-C6 cells treated by 1 mM AICAR at different time points. * $P < 0.05$ and ** $P < 0.01$ vs. untreated cells. Data are representative of three independent experiments.

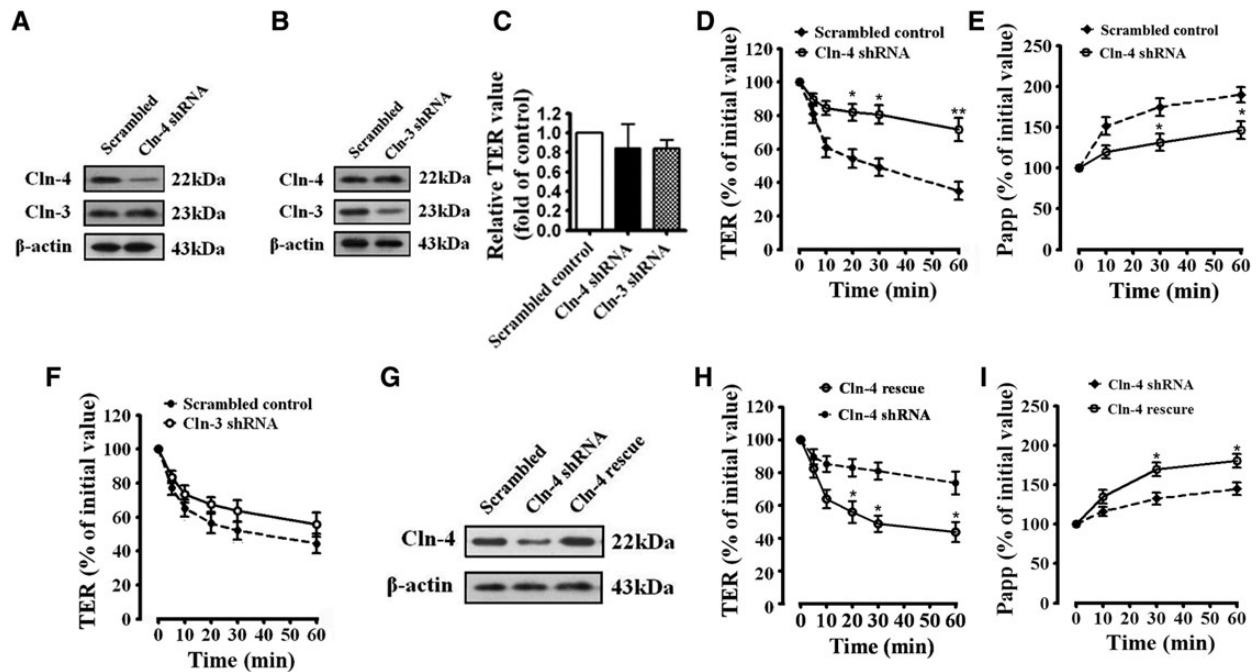


Figure 3 Claudin-4 is required to mediate AMPK-induced increase in paracellular permeability. Western blot identification of claudin-4 (A) and claudin-3 (B) in SMG-C6 cells transfected with claudin-4 and claudin-3 shRNA, respectively. (C) The basal TER values in SMG-C6 cells transfected with claudin-4 and claudin-3 shRNA, respectively. The effects of AICAR on TER in claudin-4 (D) and claudin-3 (F) knockdown SMG-C6 cells. (E) The effects of AICAR on permeability of 4 kDa FITC-dextran in claudin-4 knockdown SMG-C6 cells. * $P < 0.05$ and ** $P < 0.01$ vs. scrambled control. (G) Western blot identification of claudin-4 in the ‘rescue’ cells by transfection of claudin-4 cDNA into the claudin-4 knockdown cells. TER values (H) and permeability for 4 kDa FITC-dextran (I) in the claudin-4 ‘rescue’ cells. * $P < 0.05$ vs. claudin-4 knockdown cells. Values are mean \pm SD from three independent experiments.

knockdown cells (Figure 3D). AICAR (1 mM)-induced increase in permeability of 4 kDa FITC-dextran was also significantly inhibited in the claudin-4 knockdown cells compared with the scrambled control cells (Figure 3E). In contrast, in the claudin-3 knockdown cells, AICAR still induced a significant decline in TER values (Figure 3F).

To further confirm that the increased paracellular permeability was specifically due to claudin-4 depletion rather than other regulatory factors, we conducted a claudin-4 ‘rescue’ study by transfecting claudin-4 knockdown cells with claudin-4 cDNA. Compared with scrambled control cells, the protein level of claudin-4 was recovered to 116.1% in the claudin-4 ‘rescue’ cells (Figure 3G). Moreover, AICAR-induced TER reduction was reversed in the claudin-4 ‘rescue’ cells (Figure 3H). The permeability responses for 4 kDa dextran were also reversed in the claudin-4 ‘rescue’ cells (Figure 3I). Therefore, these results demonstrated that AMPK-induced increase in paracellular permeability was predominantly mediated through claudin-4.

Activation of AMPK increases ERK1/2 phosphorylation

We next investigated possible intracellular signaling molecules involved in the AMPK-induced alteration of TER and claudin-4 distribution. Extracellular signal-regulated kinase 1/2 (ERK1/2), p38 mitogen-activated protein kinase (p38 MAPK), and c-Jun N-terminal kinase (JNK) are major members of MAPK family. They

may play important roles in mediating expression and function of tight junction in different tissues and cells (Bell and Watson, 2013). As expected, AICAR (1 mM) increased the level of AMPK phosphorylation in SMG-C6 cells (Figure 4A). The level of p-ERK1/2 was also significantly increased after AICAR treatment for 10, 30, and 60 min, respectively (Figure 4B). However, the levels of p-p38MAPK and p-JNK did not change over the same time course (Figure 4C and D). The amount of total ERK1/2, p38MAPK, and JNK did not change by AICAR treatment for 60 min. These results suggested that ERK1/2, but not p38 MAPK or JNK, was selectively regulated by AMPK.

To explore the relationship between AMPK and ERK1/2, we respectively inhibited ERK1/2 and AMPK by usage of specific inhibitors. Pretreatment with AraA (20 μ M), an AMPK inhibitor, blocked both AMPK and ERK1/2 phosphorylation. On the other hand, 10 μ M U0126, an upstream ERK1/2 kinase inhibitor, inhibited AICAR-induced ERK1/2 phosphorylation, but had no effect on AMPK phosphorylation (Figure 4E). These data indicated that ERK1/2 was an important downstream signaling molecule of AMPK in SMG-C6 cells.

ERK1/2 is required in AMPK-modulated alteration of paracellular permeability

The involvement of ERK1/2 in AMPK-modulated paracellular permeability was further evaluated. Pretreatment with U0126 for

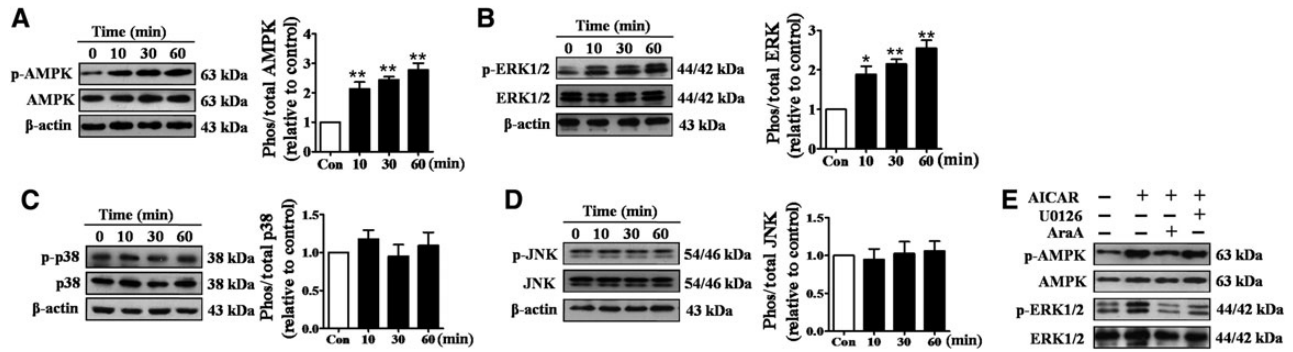


Figure 4 Activation of AMPK increases ERK1/2 phosphorylation. SMG-C6 cells were stimulated with 1 mM AICAR for 10, 30, and 60 min. Total-cell lysates were used in western blot analysis to detect the phosphorylation level of AMPK (A), ERK1/2 (B), p38 (C), and JNK (D). β -actin was used as a loading control. (E) SMG-C6 cells were stimulated with 1 mM AICAR, 10 μ M U0126, or 20 μ M AraA, alone or in combination, for 30 min as indicated. The levels of phosphorylated and total AMPK and ERK1/2 were detected by western blot analysis. * $P < 0.05$ and ** $P < 0.01$ vs. untreated control cells. Data are representative of three independent experiments.

30 min inhibited the AICAR-induced TER decrease, whereas U0126 alone had no effect on TER value (Figure 5A). Then, SMG-C6 cells were transfected with scrambled control or ERK1/2-specific siRNA. AMPK-induced increase of p-ERK1/2 was inhibited and the expression of total ERK1/2 was markedly reduced (Figure 5B). Moreover, AICAR-induced decrease in TER values was eliminated in ERK1/2 knockdown cells (Figure 5C). These results suggested that ERK1/2 activation was required in AICAR-induced alteration of paracellular permeability.

AMPK-induced redistribution of claudin-4 is dependent on ERK1/2

We further clarified whether ERK1/2 was involved in the AMPK-induced claudin-4 redistribution. The immunofluorescence analysis showed that the pretreatment with U0126 for 30 min abolishes the AMPK-induced claudin-4 redistribution, whereas U0126 alone had no effect on claudin-4 distribution (Figure 5D). Furthermore, the phenomenon that AICAR increased expression of claudin-4 in membrane and reduced claudin-4 presence in cytoplasm was blocked by pretreatment with U0126 for 30 min (Figure 5E). These results suggested that ERK1/2 was indeed required for AMPK-modulated tight junction function.

Activation of AMPK increases serine phosphorylation of claudin-4 in an ERK1/2-dependent manner

Recent studies suggest that phosphorylation of claudin-4 is required for modulation of the tight junction barrier function (Aono and Hirai, 2008). We examined claudin-4 phosphorylation in the presence of AMPK *in vitro* by immunoprecipitation. Serine phosphorylation of claudin-4 protein was significantly increased ($P < 0.01$) after AICAR treatment for 30 min (Figure 6A). However, the threonine phosphorylation in claudin-4 did not show significant difference after AICAR treatment compared with control group (Figure 6B). These results suggested that AMPK induced phosphorylation on serine residues of claudin-4 *in vitro*.

To investigate whether ERK1/2 plays an important role in AMPK-modulated claudin-4 phosphorylation, SMG-C6 cells were

pretreated with 10 μ M U0126 for 30 min and then followed by 1 mM AICAR treatment for 30 min. ERK1/2 inhibitor suppressed the AICAR-induced serine phosphorylation of claudin-4 ($P < 0.01$) (Figure 6C), but did not affect threonine phosphorylation on claudin-4 (Figure 6D). These results suggested that activation of AMPK induced serine phosphorylation on claudin-4 in an ERK1/2-dependent manner.

Serine 199 of claudin-4 is phosphorylated by AMPK

Claudin-4 contains four serine residues (Günzel and Yu, 2013). We constructed a series of claudin-4 mutants, in which the serine (S) was substituted to alanine (A), to determine the phosphorylation region required for AMPK-modulated tight junction barrier function. We overexpressed the full length wild-type claudin-4 and various phosphorylation mutants (S195A, S199A, S203A, S207A) in SMG-C6 cells. Claudin-4 phosphorylation at serine residues was elevated, respectively, in wild-type, S195A, S203A, and S207A mutant cells after AICAR stimulation, but not in S199A mutant cells (Figure 7A), which indicated that serine 199 was the phosphorylated site for AMPK activation in SMG-C6 cells.

In wild-type, S195A, S203A, or S207A claudin-4 cells, AICAR (1 mM for 60 min) still induced a significant decline in TER values. However, AICAR-induced TER decrease was significantly inhibited in S199A mutant claudin-4 cells (Figure 7B). Taken together, these results indicated that serine 199 of claudin-4 was phosphorylated by AMPK, which was required for modulation of the tight junction barrier function in SMG-C6 cells.

Activation of AMPK promotes the interaction of claudin-4 and occludin in an ERK1/2-dependent manner

Previous studies have suggested that tight junction is maintained by dynamic protein-protein interactions, which may provide a platform for rapid tight junction regulation (Shen, 2012). We evaluated the interaction between claudin-4 and occludin in response to AICAR in SMG-C6 cells. Co-immunoprecipitation studies showed that the interaction of claudin-4 and occludin was increased after 1 mM AICAR treatment for 30 min (Figure 8A). These

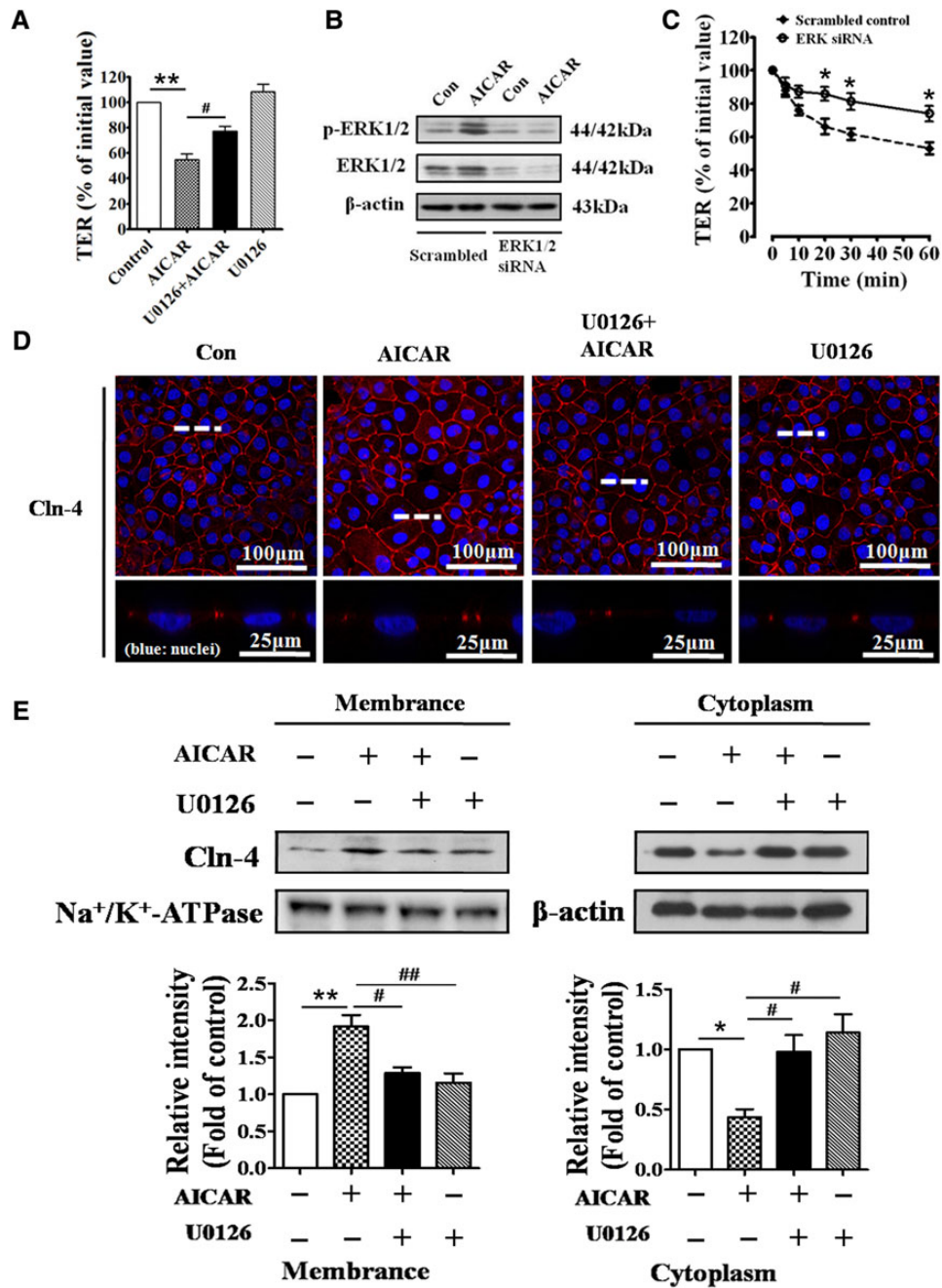


Figure 5 ERK1/2 is involved in AMPK-induced paracellular permeability and claudin-4 redistribution. (A) SMG-C6 cells were pretreatment with 10 μ M U0126 for 30 min. TER was measured by EVOM. ** $P < 0.01$ vs. control. # $P < 0.05$ vs. AICAR-treated group. (B) Expression of ERK1/2 in SMG-C6 cells transfected with ERK1/2 siRNA. (C) The effect of AICAR on TER in ERK1/2 knockdown cells. Values are mean \pm SD from three independent experiments. * $P < 0.05$ vs. cells transfected with scrambled siRNA. (D) Immunofluorescence images of claudin-4 distribution in SMG-C6 cells at x-y planes and along the z-axis after stimulation with 1 mM AICAR, 10 μ M U0126, alone or in combination, for 30 min. Each image is a representative of three separate experiments in duplicate. Scale bar, 100 and 25 μ m. (E) Western blot detecting claudin-4 expression in the membrane and cytoplasm fractions of SMG-C6 cells stimulated with 1 mM AICAR, 10 μ M U0126, alone or in combination, for 30 min. * $P < 0.05$, ** $P < 0.01$ vs. untreated cells. # $P < 0.05$, ## $P < 0.01$ vs. AICAR-treated cells. Data are representative of three independent experiments.

data suggested that AMPK activation promoted the interaction of claudin-4 and occludin.

To evaluate the role of ERK1/2 in claudin-4 and occludin interaction, SMG-C6 cells were pretreated with U0126 for 30 min.

Increased interaction of claudin-4 and occludin was inhibited (Figure 8B), which suggested that AMPK-modulated claudin-4 and occludin interaction was dependent on ERK1/2 phosphorylation.

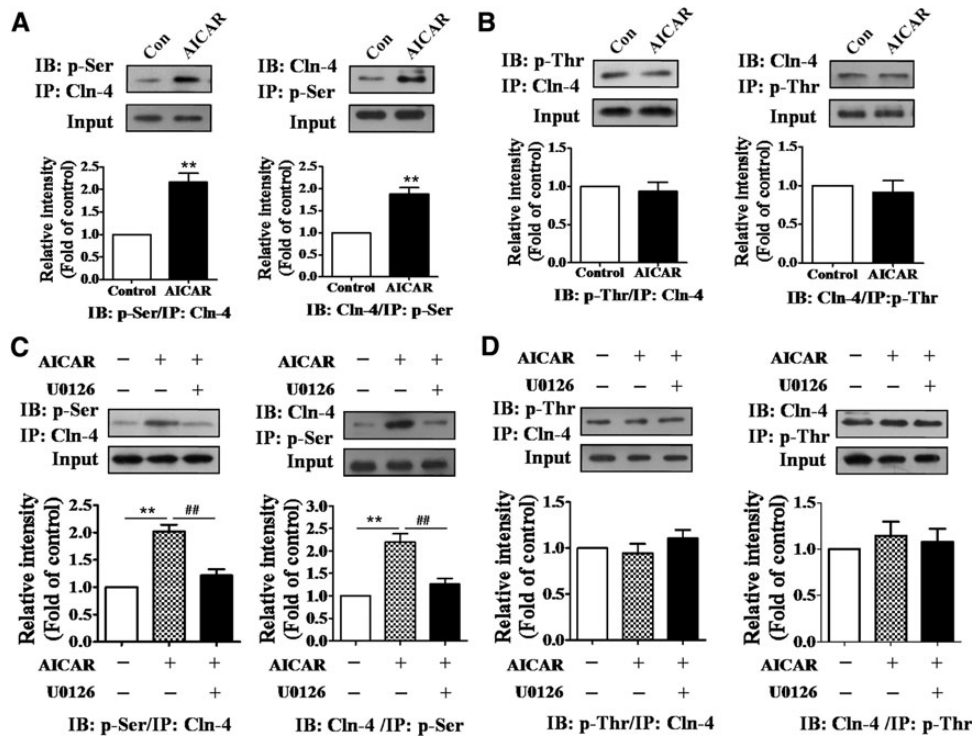


Figure 6 AMPK increases serine phosphorylation of claudin-4 dependent on ERK1/2. SMG-C6 cells were stimulated with 1 mM AICAR for 30 min. (A) The serine phosphorylation level of claudin-4 was assessed by immunoprecipitation (IP). Lysates were immunoprecipitated using anti-claudin-4 (left) or anti-phospho-Ser (right) antibody. $**P < 0.01$ vs. untreated cells. (B) The threonine phosphorylation level of claudin-4 was assessed by IP. Lysates were immunoprecipitated using anti-claudin-4 (left) or anti-phospho-Thr (right) antibody. SMG-C6 cells were pre-treated with 10 μ M U0126 for 30 min before treatment with 1 mM AICAR. (C) The serine phosphorylation level of claudin-4 was assessed by IP. Lysates were immunoprecipitated using anti-claudin-4 (left) or anti-phospho-Ser (right) antibody. $**P < 0.01$ vs. untreated cells. $##P < 0.01$ vs. AICAR-treated cells. (D) The threonine phosphorylation level of claudin-4 was assessed by IP. Lysates were immunoprecipitated using anti-claudin-4 (left) or anti-phospho-Thr (right) antibody. Data are representative of three independent experiments.

Discussion

In the present study, we demonstrated that activation of AMPK increased saliva secretion of rat submandibular glands and paracellular permeability in SMG-C6 cells. AICAR induced the redistribution of claudin-4, but not claudin-1, claudin-3, occludin, or ZO-1. By knockdown and re-expression, we revealed that claudin-4 was a required component of tight junction barrier to mediate AMPK-induced increase in paracellular permeability. Furthermore, activation of AMPK enhanced phosphorylation of claudin-4 at serine 199 and interaction of claudin-4 and occludin. ERK1/2 was responsible for AMPK-induced increase in paracellular permeability, phosphorylation, redistribution, as well as interaction of occludin and claudin-4. These results provided new insights into the crucial role of claudin-4 in forming tight junction barrier, and characterized a novel mechanism of AMPK modulating tight junction complex in submandibular epithelial cells.

SMG-C6 cells are originally derived from rat submandibular acinar cells (Quissell et al., 1997; Liu et al., 2000). Like native acinar cells, SMG-C6 cells are polarized epithelia, express tight junctions, and share intracellular structures necessary for normal acinar cell secretory function, including endoplasmic reticulum, Golgi apparatus, and secretory granules. Taken in their entirety, SMG-C6 cells are suitable for studying the role of tight junction in

regulating submandibular gland cell functions. Recent studies suggest that regulation of tight junction assembly and function involves activation of AMPK (Peng et al., 2009). Lymphocytes that are recruited to the infective sites accelerate the assembly of tight junction in epithelial cells. AMPK is required during this process in an ATP-independent manner (Tang et al., 2010). Ding et al. (2013) demonstrated that adiponectin increased saliva secretion and the width of apical tight junctions in submandibular glands by activation of adiponectin receptors and AMPK. In this study, we provided further evidence that AICAR promoted saliva secretion of rat submandibular glands, decreased TER values, and increased paracellular permeability for macromolecules in SMG-C6 cells. The results suggested that activation of AMPK might affect saliva secretion by regulating tight junction barrier function. Decreased TER was quickly recovered after AICAR removal, which also suggested that AMPK-modulated TER response might be associated with redistribution of tight junction proteins.

Claudins are the crucial structural and functional transmembrane components of tight junctions. The extracellular loops of claudins from adjacent cells interact with each other to seal the cellular sheet and regulate paracellular transport between the luminal and basolateral spaces (Krause et al., 2008). Previous studies illustrate that the distribution of individual claudins can vary and lead to

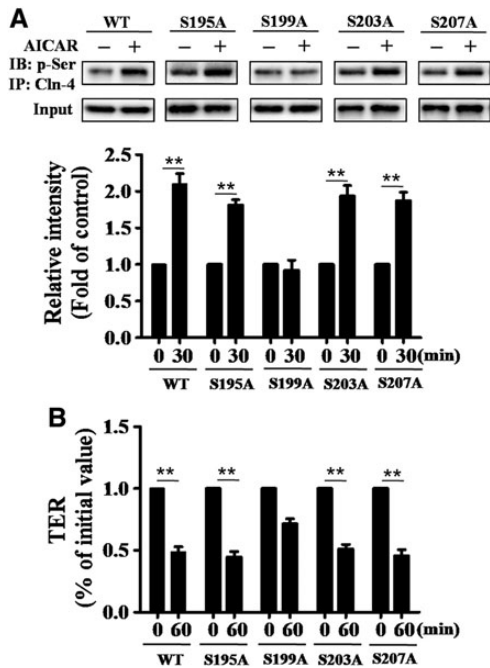


Figure 7 Serine 199 of claudin-4 is phosphorylated by AMPK. SMG-C6 cells were transfected with vectors expressing wild-type claudin-4 (WT) or mutant claudin-4 proteins (S195A, S199A, S203A, S207A). **(A)** Cells were stimulated with 1 mM AICAR for 30 min and the serine phosphorylation level of claudin-4 was assessed by IP. Data are representative of three independent experiments. **(B)** SMG-C6 cells were incubated with 1 mM AICAR for 60 min. The TER value in SMG-C6 cells transfected with WT or mutant claudin-4 proteins was measured by EVOM, respectively. $**P < 0.01$ vs. untreated cells. Values are mean \pm SD from three independent experiments.

a speculation that each claudin might be responsible for variable electrical properties of tight junctions in different tissues (Schumann et al., 2012). Theophylline induces a decrease of TER in colon tissue specimens. Western blot of membrane fraction reveals an increase of claudin-4 after theophylline incubation (Markov et al., 2014). cAMP enhances claudin-5 immunoreactivity along cell borders and induces a rapid decrease in TER via a protein kinase A-dependent pathway in porcine blood-brain barrier endothelial cells (Soma et al., 2004). *Trichomonas vaginalis* induces a decrease in TER on Caco-2 cells, which is associated with redistribution of occludin, E-cadherin, and ZO-1 proteins (da Costa et al., 2005). Recent studies indicate that claudins play important roles in AMPK-modulated tight junction barrier in epithelia. In human brain microvascular endothelial cells, high glucose reduces the level of claudin-5 that is essential for maintaining the integrity of the blood-brain barrier. AMPK activation by AICAR abolishes high glucose-induced reduction in tight junction protein expression (Liu et al., 2012). Our previous data showed that claudin-1, -3, and -4 proteins existed in SMG-C6 cells, while claudin-2 and -5 were not detected (Cong et al., 2013). Here, we further confirmed that AMPK activation induced redistribution of claudin-4 from the cytoplasm to the membrane, but did not affect the distribution of claudin-1, claudin-3, occludin, and ZO-1. These results indicate that claudin-4

might play an important role in AMPK-modulated paracellular permeability in salivary epithelium.

The previous studies have demonstrated that claudin-4 is expressed in human, rabbit, rat, and mouse submandibular glands (Lourenco et al., 2007). Peppi and Ghabriel (2004) had reported that claudin-4 selectively distributed in the striated and large excretory ducts, but not in the acini or intercalated ducts of rat parotid and submandibular glands using immunohistochemistry method. Maria et al. (2008) found that claudin-4 was expressed in both acinar and duct cells of human parotid and submandibular glands. By use of immunofluorescence method, we found that claudin-4 was mainly expressed in the duct cells and was weakly presented in acinar cells in rat submandibular glands, which suggested that claudins-4 might be involved in the regulation of barrier function in rat submandibular duct and acinar cells. However, the exact role of claudin-4 in mediating AMPK-induced alteration of paracellular permeability has not yet been elucidated. Here, we found that knockdown of claudin-4, but not claudin-3, reversed the AMPK-induced decrease in TER values and increase in paracellular flux for 4 kDa FITC-dextran, while the claudin-4 'rescue' cells restored AICAR-induced permeability responses in SMG-C6 cells. These observations demonstrated that AMPK-induced increase in paracellular permeability was predominantly mediated by claudin-4.

We next explored the signaling pathway linking AMPK activation to claudin-4. A series of studies suggested that several members of MAPK family are involved in the modulation of tight junction (Kawai et al., 2011). In Caco-2 cells, activation of ERK1/2, but not p38 MAPK or JNK, is involved in the epidermal growth factor-mediated prevention of acetaldehyde-induced increase in paracellular permeability (Samak et al., 2011). ERK1/2 is also the intracellular signaling molecule to mediate transient receptor potential vanilloid subtype 1 (TRPV1)-activated increase in paracellular tracer permeability and expression of tight junction proteins in rabbit submandibular gland (Cong et al., 2013). Therefore, MAPK might be involved in modulation of tight junction barrier in epithelium. Here, we found that the level of p-ERK1/2, but not p-p38MAPK or p-JNK, was significantly increased after AICAR stimulation. AraA blocked both AMPK and ERK1/2 phosphorylation, while U0126 only suppressed ERK1/2 phosphorylation, but had no effect on AMPK phosphorylation. These findings indicated that ERK1/2 was an important downstream signaling molecule of AMPK in SMG-C6 cells.

Increasing studies have revealed that tight junction proteins are regulated by phosphorylation, and this posttranslational modification is closely correlated with the regulation of their distribution, expression level, and biological function. Claudin-4 has four serine, one threonine and three tyrosine residues (Günzel and Yu, 2013). Atypical PKC regulates tight junction formation through the phosphorylation of claudin-4 in human epidermal keratinocytes (HaCaT) cells (Aono and Hirai, 2008). In human pancreatic cancer cells, PKC α activation downregulates tight junction functions via the phosphorylation of claudin-4 (Kyuno et al., 2011). In the present study, we found that AMPK activation selectively enhanced claudin-4 phosphorylation at serine residues, but not in threonine residues. Moreover, by constructing four serine mutants, we

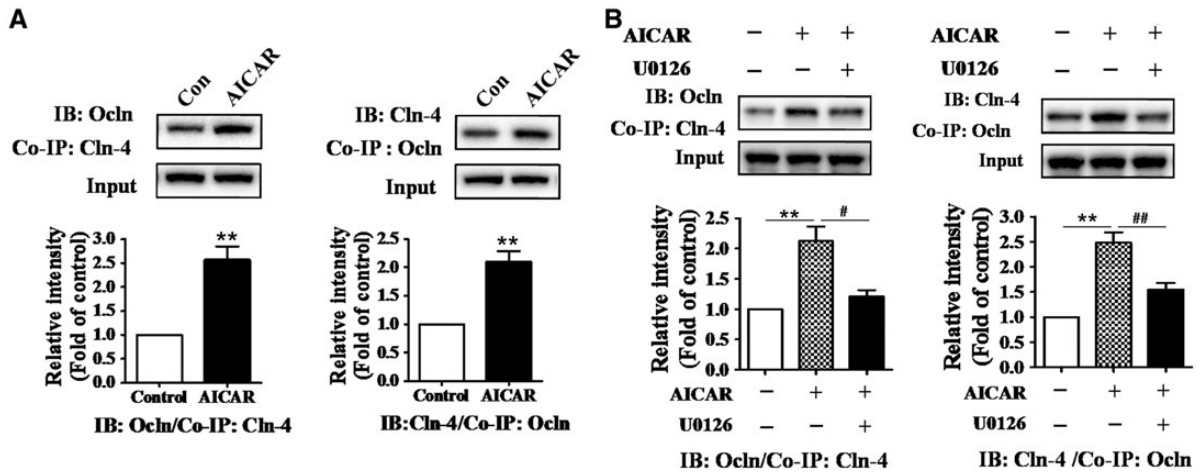


Figure 8 AICAR promotes the interaction between claudin-4 and occludin dependent on ERK1/2. **(A)** The interaction between claudin-4 and occludin was assessed by co-immunoprecipitation (co-IP). Lysates were co-immunoprecipitated using anti-claudin-4 (left) or anti-occludin (right) antibody. $**P < 0.01$ vs. untreated cells. SMG-C6 cells were pretreated with 10 μM U0126 for 30 min before 1 mM AICAR stimulation. **(B)** The interaction between claudin-4 and occludin was assessed by co-IP. Lysates were co-immunoprecipitated using anti-claudin-4 (left) or anti-occludin (right) antibody. $**P < 0.01$ vs. untreated cells. $\#P < 0.05$ and $\#\#P < 0.01$ vs. AICAR-treated cells. Data are representative of three independent experiments.

demonstrated that serine 199 of rat claudin-4, but not serine 195, 203, or 207, was the specific site phosphorylated by AMPK. In cells overexpressing S199A mutant claudin-4, AICAR-induced TER decrease was significantly inhibited. This response was not observed in wild-type, S195A, S203A, or S207A claudin-4 cells. Inhibition of ERK1/2 by pharmacological inhibitor or special siRNA suppressed the AICAR-induced TER decrease, serine phosphorylation, and redistribution of claudin-4. Taken together, these results demonstrated that serine 199 phosphorylation of claudin-4 was essential for AMPK-modulated tight junction function and ERK1/2 was the signal transduction molecule to mediate the effect of AMPK on paracellular permeability in SMG-C6 cells.

Previous reports suggested that claudins might influence the charge selectivity and electrical resistance of junctions but were not involved in the permeability of uncharged solutes (Michikawa et al., 2008). Overexpression of GFP-fused claudin-4 in SMIE cells, the rat submandibular gland epithelial cell line, significantly altered TER, but slightly affected the flux of 4-kDa dextran (Michikawa et al., 2008). However, overexpression of claudin-3 significantly altered the permeability to inorganic cations, anions, and 4-kDa dextran in MDCK II kidney tubule cells (Milatz et al., 2010). These reports suggested that effects of claudins on paracellular permeability might be dependent on different types of epithelia and stimuli. Recently, occludin has been implicated in regulation of leaky pathway flux of large macromolecules by studies of occluding knockdown, overexpression, or mutation in MDCK monolayers (Yu et al., 2005). ZO-1 can interact with both occludin and claudins. Casein kinase 2 enhanced occludin-claudin-1 and -2 interactions through ZO-1, and then promoted paracellular cation flux in Caco-2 human intestinal epithelial cells (Raleigh et al., 2011). These findings suggest that modification of interactions among tight junction proteins changed protein complex composition and stability, and these alterations might be involved in regulating the barrier function. Our results showed that the interaction of

claudin-4 and occludin was significantly enhanced in AICAR-treated SMG-C6 cells, which was abolished by ERK1/2 inhibitor. These results suggested that AMPK enhanced the interaction between claudin-4 and occludin in an ERK1/2-dependent manner, which might cause the changes to the size-selective paracellular pathway and then affect the paracellular permeability.

In summary, we demonstrated that claudin-4 played a crucial role in AMPK-modulated tight junction function in submandibular epithelium. ERK1/2 was required for AMPK-modulated serine 199 phosphorylation and redistribution of claudin-4, as well as the interaction with occludin. These findings provided a novel mechanism of AMPK modulating tight junction complex and improved our understanding of the effect on secretion of submandibular glands via paracellular pathway.

Materials and methods

Cell culture

The rat submandibular gland cell line SMG-C6 (a gift kindly from Dr David O. Quissell) were cultured in DMEM/F12 (1:1 mixture) medium containing 2.5% fetal bovine serum, 5 $\mu\text{g/ml}$ transferrin, 1.1 $\mu\text{mol/L}$ hydrocortisone, 0.1 $\mu\text{mol/L}$ retinoic acid, 2 nmol/L thyronine T_3 , 5 $\mu\text{g/ml}$ insulin, 80 ng/ml epidermal growth factor, 50 $\mu\text{g/ml}$ gentamicin sulfate, 5 mmol/L glutamine, 100 U/ml penicillin, and 100 $\mu\text{g/ml}$ streptomycin in 5% CO_2 . All constituents used in culturing SMG-C6 cells were purchased from Sigma-Aldrich Co. In some experiments, the cells were incubated in K^+ -free Krebs solution (142.4 mM NaCl, 2.8 mM CaCl_2 , 0.6 mM NaH_2PO_4 , 1.2 mM MgSO_4 , 10 mM glucose, 15 mM Tris, pH 7.4) for 30 min and then exposed to 1 mM AICAR.

Perfusion of rat submandibular glands

Healthy male Sprague Dawley (SD) rats (250–350 g) were obtained from Peking University Health Science Center. All experimental procedures were approved by the Peking University Institutional

Review Board, for the care and use of laboratory animals.

Briefly, SD rats underwent surgery under deep isoflurane anesthesia (3%). Submandibular glands were isolated and perfused through a polyethylene cannula placed in the external carotid artery. The main excretory duct was annulated for saliva collection. The glands were perfused arterially in KRH buffer (KRH, 116 mM NaCl, 5.4 mM KCl, 1.25 mM CaCl₂, 0.4 mM MgSO₄, 20 mM HEPES, 0.9 mM Na₂HPO₄, and 5.6 mM glucose, pH 7.4) for 30 min at a rate of 1.8 ml/min with a Gilson Minipuls rotary pump. After equilibration for at least 30 min, different stimulators ($n = 3$ for each group) were perfused into the glands for 30 min, respectively. The secretion of the glands was measured as the length of moisture on the filter paper (35 mm × 5 mm) after perfusion of drugs.

Western blot analysis

Cells were lysed in an ice-cold lysis buffer. Equal amounts of proteins (40 µg) were separated by 12% SDS-PAGE and transferred to polyvinylidene difluoride membrane. Primary antibody-probed blots were visualized with appropriate horseradish peroxidase-coupled secondary antibodies using enhanced chemiluminescence reagent. The densities of bands were quantified with the Image J Software (National Institutes of Health, MD, USA). Actin was used as a loading control for standardization of blots.

Immunofluorescence staining

The SMG-C6 cells grown on glass coverslips were fixed in 4% paraformaldehyde in PBS for 15 min, permeabilized with 0.1% Triton X-100 for 3 min, blocked with 5% BSA for 30 min, and then, the cells were stained with TRITC-labeled claudin-4 for 2 h at 37°C. The cells were also stained with antibodies for claudin-3 or claudin-1 at 4°C overnight, and then incubated with TRITC-labeled secondary antibody for 2 h at 37°C. Nuclei were labeled with 4, 6-diamidino-2-phenylindole (DAPI). Fluorescence images were taken with a confocal microscope (Leica TCS SP5).

Preparation of cytoplasm and membrane fractions

Cell monolayers cultured were exposed to various treatments and subsequently subjected to an extraction protocol adapted from Kawedia et al. (2008). Briefly, cells were lysed in ice-cold 0.5% Triton X-100, 100 mM NaCl, 10 mM Tris-HCl (pH 7.4), and 300 mM sucrose for 20 min at 4°C. The Triton X-100-soluble (cytoplasm fraction) fraction was completely removed and the remaining, insoluble residue was again lysed (membrane fraction) in 50 mM Tris (pH 6.8), 2% SDS, and 10% glycerol.

TER measurement and non-selective monolayer permeability assay

TER of SMG-C6 cells grown on 24-well Transwell™ chambers (polycarbonate membrane, filter pore size: 0.4 µm; filter area: 0.33 cm²; Costar) were measured by using an epithelial volt ohm meter (EVOM; World Precision Instruments). The value of the blank filter (90 Ω) was subtracted, and all measurements were performed on a minimum of triplicate wells. The 4 kDa FITC-dextran was added apically and samples were collected from the basal side after 10 min of 1 mM AICAR treatment. Using a fluorometer

(BioTek), apparent permeability coefficients (Papp) were calculated as the increase in the tracer amount per time and per filter area (Rosenthal et al., 2010).

Knockdown of claudin-3, claudin-4, and ERK1/2

The shRNAs of claudin-3 and claudin-4 were produced by Origene Technologies (Origene). The oligoribonucleotides were 5'-ACGG CACACAACGTCATCCGCGACTTCTA-3' (claudin-4 shRNA) and 5'-CTCTC ATCGTGGTGTCTATCCTACTGGCA-3' (claudin-3 shRNA). The potent rat ERK1/2 siRNA sequence 5'-GACCGAUGUUAACCUUUUUAUUTT-3' and non-specific control were synthesized by GeneChem. SMG-C6 cells were cultured to 80% confluence and transfected with siRNA or shRNA of interests by use of MegeTran 1.0 (Origene) according to the manufacturer's instructions.

Re-expression of claudin-4

Claudin-4 re-expression ('rescue') was carried out by generating a Myc-tagged cDNA clone of claudin-4 in a pCMV6 vector (Origene). Plasmid transfection was performed by use of MegeTran 1.0 and the ratio of transfection reagent to DNA was 3:1 as described in the manufacturer's instructions. The cells were collected at 24 h post-transfection.

Immunoprecipitation and co-immunoprecipitation

SMG-C6 cells were plated at 80%–90% confluence in 60 mm dishes. Cells were stimulated with AICAR (1 mM) for 30 min. The cell lysates were prepared with protease inhibitors in BSA buffer (50 mM Tris-HCl, pH 7.5, 15 mM EGTA, 100 mM NaCl, 1 mM DTT, 1 mM phenylmethanesulfonyl fluoride, 100 mM NaF, 1 mM Na₃VO₄, and 0.1% Triton X-100). Cell lysates were incubated with protein A/G-agarose (Santa Cruz Biotechnology, Santa Cruz) for 1 h at 4°C and then clarified by centrifugation at 15000 *g* for 10 min. The supernatants were incubated with the polyclonal anti-claudin-4, anti-occludin, anti-phosphoserine, and anti-phosphothreonine antibodies bound to protein A/G overnight at 4°C. After incubation, immunoprecipitates were washed extensively with the same lysis buffer and subjected to western blot analysis.

Statistical analysis

Data are presented as means ± SD. Statistical analysis for multiple groups involved one-way followed by Bonferroni's test or two-way ANOVA using GraphPad software (GraphPad Prism). Values of $P < 0.05$ were considered statistically significant (* $P < 0.05$ and ** $P < 0.01$; # $P < 0.05$ and ## $P < 0.01$).

Acknowledgements

We thank Dr David O. Quissell (School of Dentistry, University of Colorado Health Sciences Center, Denver, CO, USA) for the generous gift of rat SMG-C6 cell line.

Funding

This study was supported by grants from the National Natural Science Foundation of China (no. 81100763, 81271161, and 81442007).

Conflict of interest: none declared.

References

- Aono, S., and Hirai, Y. (2008). Phosphorylation of claudin-4 is required for tight junction formation in a human keratinocyte cell line. *Exp. Cell Res.* *314*, 3326–3339.
- Bell, C.E., and Watson, A.J. (2013). p38 MAPK regulates cavitation and tight junction function in the mouse blastocyst. *PLoS One* *8*, e59528.
- Claverie-Martin, F., García-Nieto, V., Loris, C., et al. (2013). Claudin-19 mutations and clinical phenotype in Spanish patients with familial hypomagnesemia with hypercalciuria and nephrocalcinosis. *PLoS One* *8*, e53151.
- Cong, X., Zhang, Y., Yang, N.Y., et al. (2013). Occludin is required for TRPV1-modulated paracellular permeability in the submandibular gland. *J. Cell Sci.* *126*(Pt 5), 1109–1121.
- da Costa, R.F., de Souza, W., Benchimol, M., et al. (2005). *Trichomonas vaginalis* perturbs the junctional complex in epithelial cells. *Cell Res.* *15*, 704–716.
- Ding, C., Li, L., Su, Y.C., et al. (2013). Adiponectin increases secretion of rat submandibular gland via adiponectin receptors-mediated AMPK signaling. *PLoS One* *8*, e63878.
- Egawa, M., Kamata, H., Kushiya, A., et al. (2008). Long-term forskolin stimulation induces AMPK activation and thereby enhances tight junction formation in human placental trophoblast BeWo cells. *Placenta* *29*, 1003–1008.
- Ewert, P., Aguilera, S., Alliende, C., et al. (2010). Disruption of tight junction structure in salivary glands from Sjögren's syndrome patients is linked to proinflammatory cytokine exposure. *Arthritis Rheum.* *62*, 1280–1289.
- Frigeri, A., Nicchia, G.P., and Svelto, M. (2007). Aquaporins as targets for drug discovery. *Curr. Pharm. Des.* *13*, 2421–2427.
- Furuse, M., Hata, M., Furuse, K., et al. (2002). Claudin-based tight junctions are crucial for the mammalian epidermal barrier: a lesson from claudin-1-deficient mice. *J. Cell Biol.* *156*, 1099–1111.
- Günzel, D., and Fromm, M. (2012). Claudins and other tight junction proteins. *Compr. Physiol.* *2*, 1819–1852.
- Günzel, D., and Yu, A.S. (2013). Claudins and the modulation of tight junction permeability. *Physiol. Rev.* *93*, 525–569.
- Kawai, Y., Hamazaki, Y., Fujita, H., et al. (2011). Claudin-4 induction by E-protein activity in later stages of CD4/8 double-positive thymocytes to increase positive selection efficiency. *Proc. Natl Acad. Sci. USA* *108*, 4075–4080.
- Kawedia, J.D., Nieman, M.L., Boivin, G.P., et al. (2007). Interaction between transcellular and paracellular water transport pathways through Aquaporin 5 and the tight junction complex. *Proc. Natl Acad. Sci. USA* *104*, 3621–3626.
- Kawedia, J.D., Jiang, M., Kulkarni, A., et al. (2008). The protein kinase A pathway contributes to Hg²⁺-induced alterations in phosphorylation and subcellular distribution of occludin associated with increased tight junction permeability of salivary epithelial cell monolayers. *J. Pharmacol. Exp. Ther.* *326*, 829–837.
- Kottakis, F., and Bardeesy, N. (2012). LKB1-AMPK axis revisited. *Cell Res.* *22*, 1617–1620.
- Krause, G., Winkler, L., Mueller, S.L., et al. (2008). Structure and function of claudins. *Biochim. Biophys. Acta* *1778*, 631–645.
- Kyuno, D., Kojima, T., Ito, T., et al. (2011). Protein kinase C α inhibitor enhances the sensitivity of human pancreatic cancer HPAC cells to Clostridium perfringens enterotoxin via claudin-4. *Cell Tissue Res.* *346*, 369–381.
- Liu, X.B., Sun, X., Mork, A.C., et al. (2000). Characterization of the calcium signaling system in the submandibular cell line SMG-C6. *Proc. Soc. Exp. Biol. Med.* *225*, 211–220.
- Liu, C., Wu, J., and Zou, M.H. (2012). Activation of AMP-activated protein kinase alleviates high-glucose-induced dysfunction of brain microvascular endothelial cell tight-junction dynamics. *Free Radic. Biol. Med.* *53*, 1213–1221.
- Lourenco, S.V., Coutinho-Camillo, C.M., Buim, M.E., et al. (2007). Human salivary gland branching morphogenesis: morphological localization of claudins and its parallel relation with developmental stages revealed by expression of cytoskeleton and secretion markers. *Histochem. Cell Biol.* *128*, 361–369.
- María, O.M., Kim, J.W., Gerstenhaber, J.A., et al. (2008). Distribution of tight junction proteins in adult human salivary glands. *J. Histochem. Cytochem.* *56*, 1093–1098.
- Markov, A.G., Falchuk, E.L., Kruglova, N.M., et al. (2014). Comparative analysis of theophylline and cholera toxin in rat colon reveals an induction of sealing tight junction proteins. *Pflugers Arch.* *466*, 2059–2065.
- Michikawa, H., Fujita-Yoshigaki, J., and Sugiya, H. (2008). Enhancement of barrier function by overexpression of claudin-4 in tight junctions of submandibular gland cells. *Cell Tissue Res.* *334*, 255–264.
- Milatz, S., Rosenthal, R., et al. (2010). Claudin-3 acts as a sealing component of the tight junction for ions of either charge and uncharged solutes. *Biochim. Biophys. Acta* *1798*, 2048–2057.
- Muto, S., Hata, M., Taniguchi, J., et al. (2010). Claudin-2-deficient mice are defective in the leaky and cation-selective paracellular permeability properties of renal proximal tubules. *Proc. Natl Acad. Sci. USA* *107*, 8011–8016.
- Paris, L., Tonutti, L., Vannini, C., et al. (2008). Structural organization of the tight junctions. *Biochim. Biophys. Acta* *1778*, 646–659.
- Peng, L., Li, Z.R., Green, R.S., et al. (2009). Butyrate enhances the intestinal barrier by facilitating tight junction assembly via activation of AMP-activated protein kinase in Caco-2 cell monolayers. *J. Nutr.* *139*, 1619–1625.
- Peppi, M., and Ghabriel, M.N. (2004). Tissue-specific expression of the tight junction proteins claudins and occludin in the rat salivary glands. *J. Anat.* *205*, 257–266.
- Quissell, D.O., Barzen, K.A., Gruenert, D.C., et al. (1997). Development and characterization of SV40 immortalized rat submandibular acinar cell lines. *In Vitro Cell. Dev. Biol. Anim.* *33*, 164–173.
- Raleigh, D.R., Boe, D.M., and Yu, D. (2011). Occludin S408 phosphorylation regulates tight junction protein interactions and barrier function. *J. Cell Biol.* *193*, 565–582.
- Rosenthal, R., Milatz, S., Krug, S.M., et al. (2010). Claudin-2, a component of the tight junction, forms a paracellular water channel. *J. Cell Sci.* *123*, 1913–1921.
- Sáenz-Morales, D., Conde, E., Escribese, M.M., et al. (2009). ERK1/2 mediates cytoskeleton and focal adhesion impairment in proximal epithelial cells after renal ischemia. *Cell. Physiol. Biochem.* *23*, 285–294.
- Samak, G., Aggarwal, S., and Rao, R.K. (2011). ERK is involved in EGF-mediated protection of tight junctions, but not adherens junctions, in acetaldehyde-treated Caco-2 cell monolayers. *Am. J. Physiol. Gastrointest. Liver Physiol.* *301*, G50–G59.
- Schumann, M., Kamel, S., Pahlitzsch, M.L., et al. (2012). Defective tight junctions in refractory celiac disease. *Ann. NY Acad. Sci.* *1258*, 43–51.
- Shang, X., Lin, X., Alvarez, E., et al. (2012). Tight junction proteins claudin-3 and claudin-4 control tumor growth and metastases. *Neoplasia* *14*, 974–985.
- Shen, L. (2012). Tight junctions on the move: molecular mechanisms for epithelial barrier regulation. *Ann. NY Acad. Sci.* *1258*, 9–18.
- Ship, J.A. (2002). Diagnosing, managing, and preventing salivary gland disorders. *Oral Dis.* *8*, 77–89.
- Söderman, J., Norén, E., Christiansson, M., et al. (2013). Analysis of single nucleotide polymorphisms in the region of CLDN2-MORC4 in relation to inflammatory bowel disease. *World J. Gastroenterol.* *19*, 4935–4943.
- Soma, T., Chiba, H., Kato-Mori, Y., et al. (2004). Thr207 of claudin-5 is involved in size-selective loosening of the endothelial barrier by cyclic AMP. *Exp. Cell Res.* *300*, 202–212.
- Tang, X.X., Chen, H., Yu, S., et al. (2010). Lymphocytes accelerate epithelial tight junction assembly: role of AMP-activated protein kinase (AMPK). *PLoS One* *5*, e12343.
- Yu, A.S., McCarthy, K.M., Francis, S.A., et al. (2005). Knockdown of occludin expression leads to diverse phenotypic alterations in epithelial cells. *Am. J. Physiol. Cell Physiol.* *288*, C1231–C1241.
- Zhang, L., Li, J., Young, L.H., et al. (2006). AMP-activated protein kinase regulates the assembly of epithelial tight junctions. *Proc. Natl Acad. Sci. USA* *103*, 17272–17277.